Cellulose (2014) 21:2599–2609
DOI 10.1007/s10570-014-0341-0

ORIGINAL PAPER

From paper to nanopaper: evolution of mechanical and physical properties

I. González · M. Alcalà · G. Chinga-Carrasco · F. Vilaseca · S. Boufi · P. Mutjé

Received: 19 February 2014 / Accepted: 20 June 2014 / Published online: 2 July 2014

Abstract In the present work the evolution of physical and mechanical properties of papers and nanopapers is studied. Handsheets made of eucalyptus fibres reinforced with 0, 25, 50, 75 and 100 wt% of nanofibrillated cellulose (NFC) content were fabricated using a Rapid Köthen-like equipment. The obtained papers and nanopapers were physical- and mechanically-characterized. The results showed a significant increase in density and a reduction of porosity in the samples during their transition from paper to nanopaper; besides, nanopapers were more transparent and smoother than normal papers. These physical changes where more evident with increasing amounts of NFC. Regarding mechanical properties, nanopapers with a 100 wt% content of NFC improved their strength and rigidity in 228 and 317 %, respectively, in comparison with normal papers. The evolution of strength and rigidity from paper to nanopaper was linear in relation to the amount of NFC, which means that the ultimate tensile strength was mainly dependant on nanofibril failure.

Keywords Nanofibrillated cellulose · Nanopaper · Eucalyptus pulp · Mechanical properties · Physical properties

I. González (✉) · F. Vilaseca · P. Mutjé
Group LEPAMAP, Department of Chemical Engineering, University of Girona, c/M. Aurèlia Campmany, no 61, 17071 Gerona, Spain
e-mail: israel.gonzalez@udg.edu

M. Alcalà
PRODIS Group, Department of Organization, Business Management and Product Design, University of Girona, EPS Campus Montilivi, 17071 Gerona, Spain

G. Chinga-Carrasco
Paper and Fibre Research Institute (PFI), Hogskoleringen 6b, 7491 Trondheim, Norway

S. Boufi
Laboratoire des Sciences des Matériaux et Environment, Faculté des Sciences de Sfax, Université de Sfax, Sfax, Tunisia

Introduction

The interest for the production and application of nanofibrillated cellulose (NFC) has kept increasing during the last years (Siró and Plackett 2010). Their low weight, abundance, biodegradability and renewability, combined with high strength and rigidity make them interesting materials for reinforcing different polymeric matrices, including cellulose itself. In addition to these properties, NFC presents the ability to form networks of great strength within the matrix through hydrogen-bonding (Yano and Nakahara 2004; Henriksson et al. 2011). The resulting nanocomposites present improved mechanical strength, barrier properties, transparency and biodegradability. The structure of normal paper can be described as a network of cellulose fibres intertwined among them and held

together by mechanical and hydrogen bonds. The strength of paper is usually improved by the papermaking industry through mechanical treatments that tend to defibrillate the cellulose fibres, thus increasing the specific surface area of the fibres and promoting the formation of more hydrogen bonds (Carrasco et al. 1996). However, the use of NFC as paper additive to enhance mechanical properties has only been slightly explored. Its addition on papermaking slurries improves strength, increases density and reduces porosity of the ensuing paper (González et al. 2012). Nevertheless, deterioration in draining capacity of papermaking slurries has been argued as a drawback for NFC-reinforced papers (Ahola et al. 2008; Taipale et al. 2010; González et al. 2012, 2013a, b). This phenomenon limits the amount of NFC that can be added to the paper suspensions. The fabrication of films or sheets made completely of NFC (nanopaper) has also been explored. These films have been produced either by casting of a diluted NFC water suspension and evaporation of water at room temperature or in an oven (Dufresne et al. 1997; Andresen et al. 2007; Chinga-Carrasco 2013), or by vacuum filtering of the same dilution (Henriksson et al. 2008; Nogi et al. 2009; Sehaqui et al. 2010; Chun et al. 2011; Österberg et al. 2013; Varanasi and Batchelor 2013). In the case of filtering, a subsequent drying step becomes necessary to eliminate the humidity of the resulting NFC mat. The nanopapers obtained are reported like transparent rigid films with high strength and good barrier properties. These characteristics make nanopapers excellent materials for applications on electronic devices (Fang et al. 2013). In that work, the authors reported the fabrication of highly transparent, nanostructured paper with varying contents of NFC. Such hybrid nanopapers were used as a physical support to carbon nanotubes for the fabrication of touchscreens. One of the main drawbacks found in the different approaches for the fabrication of nanopapers is the long time required to drain the water from the suspension (Österberg et al. 2013). Draining times reported vary from several hours to a few days if we also consider the drying step. This disadvantage becomes unfeasible from a commercial point of view. However, several authors have recently reported an important reduction of the overall time of fabrication of a single nanopaper sheet (Österberg et al. 2013; Varanasi and Batchelor 2013). Even though there is a growing amount of published articles about the fabrication, properties and possible uses of nanopapers, the evolution of mechanical and physical properties from papers with 0 wt% of NFC until 100 wt% of NFC has not been fully studied. In the present work we study the evolution of physical and mechanical properties from papers with 100 % content of bleached eucalyptus fibres to 100 % tetramethylpiperidine-1-oxyl radical (TEMPO)–NFC from the same bleached pulp, with intermediates of 25, 50 and 75 % content of NFC.

Materials and methods

Materials

Commercial dried bleached Eucalyptus pulp from La Montañanesa (Grupo Torraspapel, Zaragoza, Spain) was used as starting material for the preparation of NFC. For the oxidation process prior to defibrillation, 2,2,6,6-tetramethylpiperidine-1-oxyl radical (TEMPO), sodium bromide (NaBr), sodium chlorite ($NaClO_2$) and sodium hypochlorite solution (NaClO) were acquired from Sigma-Aldrich and used as received.

Methods

Preparation of NFC

The TEMPO-mediated oxidation of cellulose fibres was carried out at neutral pH conditions according to methodology reported elsewhere (Besbes et al. 2011; Alila et al. 2013). In a typical experiment, five grams of cellulose fibres were suspended in 0.05 M sodium phosphate buffer solution (500 mL, pH 7) that contained TEMPO (25 mg) and NaBr (250 mg). Magnetic stirring was applied to the suspension in order to assure good dispersion of all the substances. $NaClO_2$ solution (1.13 g, 10 mM) and NaClO (0.5 mL, of a 2 M solution, 1.0 mM) were added to the suspension, stirring at 500 rpm and 60 °C during 2 h. Oxidation was then stopped by adding 100 mL of ethanol. The oxidized fibres were next washed with distilled water two times and then filtered. Finally, the fibre suspension was cooled at room temperature before proceeding to the mechanical treatment. The fibrillation process was performed by passing a 1–2 wt% fibre-water suspension through a high-pressure homogenizer (NS1001L PANDA 2K-GEA).

The equipment operated at 600 bar pressure and 60–70 °C. The process was repeated several times until a transparent, gel-like product was obtained.

Characterization of NFC

The degree of polymerization (DP) was determined from intrinsic viscosity measurements, according to UNE 57-039-92. The viscosimetric average molecular weight was calculated from the next equation: $\eta = K \cdot M^a$, where η is the intrinsic viscosity, $K = 2.28$ and $a = 0.76$ (Henriksson et al. 2008). The water retention value (WRV) was measured by separating a determined volume of NFC gel into 2 equal portions, which were then centrifuged in a Sigma Laborzentrifugen model 6K15 at 2,400 rpm for 30 min to eliminate non-bonded water. In order to retain the NFC, a nitrocellulose membrane with a pore of 0.65 μm diameter was used at the bottom of the centrifuge bottles. Once centrifuged, only the NFC in contact with the membrane was removed, weighted and then dried at 105 ± 2 °C for 24 h in containers of previously measured weight. This methodology is based on TAPPI UM 256. The average WRV value was then calculated according to the next equation:

$$WRV\,(\%) = \frac{Ww - wd}{Wd} \times 100 \qquad (1)$$

where Ww is the wet weight (g), Wd the dry weight (g). The carboxyl content (CC) of TEMPO-oxidized cellulose was calculated by conductometric titration. A dried sample (50–100 mg) was suspended in 15 mL of 0.01 M HCl solution; this exchanges Na cations bound to the COOH group by H ions. After 10 min of magnetic stirring, the suspensions were titrated with 0.01 M NaOH, adding 0.1 mL of NaOH to the suspension and then recording the conductivity in mS/cm; this process was repeated until observing a reduction, stabilization and increasing in the conductivity. From the conductometric titration curve the presence of strong and weak acid is observed. The CC is given by the following equation:

$$CC = 162(V_2 - V_1)c[(w - 36)(V_2 - V_1)c]^{-1} \qquad (2)$$

where V1 and V2 are the equivalent volumes of added NaOH solution (L), c is the NaOH concentration (mol/L), and w the weight of oven-dried sample (g). The results indicate the average mmols of –COOH groups per gram of NFC. The cationic demand of NFC was also determined by means of a Mütek PCD 04 particle charge detector. First, 0.04 g of NFC (dried weight) was diluted in 1 L distilled water and dispersed with a pulp disintegrator during 10 min at 3,000 rpm. Afterwards, 10 mL were taken and mixed with 25 mL of cationic polymer polydiallyldimethylammonium chloride (polyDADMAC) for 5 min with magnetic stirring. After this time the mixture was centrifuged in a Sigma Laborzentrifugen model 6K 15 during 90 min at 4,000 rpm. Then, 10 mL of the supernatant were taken to the Mütek equipment. Anionic polymer (Pes-Na) was then added to the sample drop by drop with a pipette until the equipment reaches 0 mV. The volume of anionic polymer consumed was used to calculate the cationic demand through Eq. 3:

$$CD = -\frac{(C_{PolyD} \cdot V_{PolyD})(V_{Pes-Na} \cdot C_{Pes-Na})}{W_{sample}} \qquad (3)$$

where CD is the cationic demand (μeq/L), C_{PolyD} = cationic polymer concentration (g/L), V_{PolyD} = used volume of cationic polymer (mL), $C_{Pes\text{-}Na}$ = anionic polymer concentration (g/L), $V_{Pes\text{-}Na}$ = used volume of anionic polymer (mL) and W_{sample} = sample's dry weight (g). The yield in NFC was also determined; a NFC suspension with 0.2 % of solid content was centrifuged at 4,500 rpm during 20 min in order to isolate the nanofibrillated fraction (contained in the supernatant) from the non-fibrillated and partially fibrillated one retained in the sediment fraction which is recovered, weighted and oven-dried at 90 °C until constant weight. The yield of nanofibrillation is then calculated from the next equation:

$$\text{Yield}\% = \left(1 - \frac{\text{weight of dried sediment}}{\text{weight of diluted sample} \times \%Sc}\right) \times 100 \qquad (4)$$

where %Sc represents the solid content of the diluted gel sample.

Transmittance measurements were performed on NFC suspensions with 0.1 % of solid content. The sample was introduced in quartz cuvettes and the transmittance measured with a UV–Vis Shimadzu spectrophotometer UV-160A set in the range between 400 and 800 nm. Distilled water was used as reference.

Fabrication of nanopaper

Slurries with 0, 25, 50, 75 and 100 wt% content of NFC against eucalyptus fibres were prepared by dispersing the required amount of NFC and fibres in 2 L of distilled water and dispersed in a pulp disintegrator at 180,000 revolutions. The NFC slurry was then vacuum-dewatered in a Rapid Köthen-like sheet former equipment. The screen in the stock container was provided with a 0.65 μm nitrocellulose filter membrane to retain the NFC. The sheet former operated at −0.4 bars of pressure. The slurry was left to dewater until a mat of NFC gel was observed at the bottom of the stock container. The thus obtained nanopaper sheets were then put between two absorbing sheets and vacuum dried during 15–20 min in a Rapid–Köthen sheet formator (ISP mod. 786 FH) according to ISO 5269-2. Finally, the handsheets were conditioned in a weather chamber at 25 °C and 50 % humidity for 24 h before mechanical testing.

Mechanical and physical characterization of nanopapers

Nanopaper samples were mechanically tested in an Instron universal testing machine provided with 2.5 kN load cell. Distance between clamps was set at 150 mm. Preload was 0.1 N and cross-head speed 15 mm/min. The testing specimens were cut down to stripes of 20 mm length and 15 mm width. The results obtained were the average of at least 5 tested samples. Density was calculated from the basis weight, thickness and dimensions of the handsheets. Porosity was determined from the density of the biocomposite by applying the next equation:

$$Porosity\,(\%) = 100 \cdot \left(1 - \frac{\rho_{sample}}{\rho_{cellulose}}\right) \quad (5)$$

where ρ_{sample} is the density of the biocomposites and and $\rho_{cellulose}$ is the density of crystalline cellulose, assumed to be 1.6 g/cm^3 (Henriksson et al. 2011; Saito et al. 2013). The roughness of the nanopaper samples was studied through laser profilometry. Samples of 10 mm × 10 mm were coated with a layer of gold for LP analysis (Lehmann, Lehman Mess-Systeme AG, Baden-Dättwil, Germany). Ten LP topography images were acquired from the top side of each sample. The lateral and z-resolution of the LP system was 1 μm and 10 nm, respectively. The size of the local areas was 1 mm × 1 mm. The surfaces were horizontally levelled. The surface images were bandpass filtered to suppress the surface structures with wavelengths larger than approximately 160 μm, applying a FFT filter implemented in the ImageJ program. The roughness described by the root-mean square (Sq) was thus quantified at wavelengths of <160 μm (Chinga-Carrasco et al. 2013).

Scanning electron microscopy (SEM)

The microscope was a Hitachi S-3000 variable pressure SEM (Hitachi High-Technologies Corporation, Minatoku, Tokyo, Japan). SEM surface images were acquired at 50× and 1,000× magnifications, in secondary electron imaging mode. The acceleration voltage and working distance were 5 kV and 12 mm, respectively.

Atomic force microscopy (AFM)

The AFM imaging was performed in a Multimode AFM (with Nanoscope V controller), Digital Instruments. All images were recorded in ScanAsyst mode (peak force tapping mode), at room temperature in air. The AFM tips of spring constant value ∼0.4 N/m was purchased from Bruker AFM probes. The size of the assessed areas was 2 μm × 2 μm. AFM imaging was performed only on the sample with 100 wt% content of NFC.

Results and discussion

Characterization of NFC

The DP, WRV, cationic demand and CC of NFC were characterized. The average DP was determined to be 423. The DP is directly related to the ultimate tensile strength of nanopapers (Henriksson et al. 2008; Chun et al. 2011); the relation between the DP of our NFC and the tensile strength of produced nanopapers are in accordance with the results reported by Henriksson et al. (2008), though nanopapers in that study were fabricated following a different methodology. The WRV, which is a measure of the capacity of a test pad of fibres to hold water, NFC presented an average of 17 g/g. This value is superior than those seen in larger

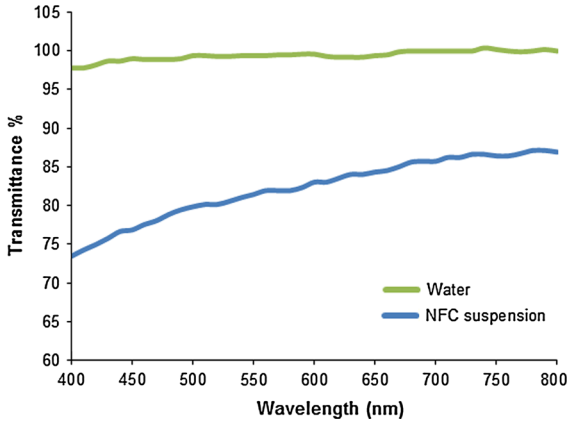

Fig. 1 UV–Vis transmittance spectra of the NFC suspension and water as a reference

fibres submitted to mechanical beating. Dang et al. (2007) also found an increase in the WRV of fibres after TEMPO-mediated oxidation of softwood bleached Kraft pulp. Regarding cationic demand, NFC presented a value of 859 μeq g/g. Cellulose fibres become negative when suspended in water due to the ionisation of carboxylic groups and to the absorption of some ions in the water (Mutjé et al. 2006). Fibrillation leads to a larger specific surface area of fibres due to cell-wall delamination, which increases the cationic demand. The content of carboxyl groups of NFC samples was 0.4 mmol/g. This parameter is the main factor that determines the extent of the nanofibrillation (Besbes et al. 2011) and the DP (Isogai et al. 2011). The level of fibrillation of the NFC was studied using UV–Vis transmittance and yield of fibrillation. The first technique refers to the transmittance of a NFC aqueous suspension measured by UV–Vis spectrophotometer. The transmittance is wavelength-dependant because light scatters more when the wavelength approaches the diameter of the particles (Saito et al. 2007). Highly fibrillated fibres produce spectra where the transmittance is close to 100 % (Saito et al. 2007; Besbes et al. 2011). Figure 1 shows the spectrum of the NFC suspension used during the present work; distilled water was used as a reference.

The carboxylic content and the intensity of the mechanical treatment greatly influence the transmittance of the NFC suspensions (Besbes et al. 2011). Though higher content of COOH groups would have produced more transparent NFC suspensions, the resulting depolymerisation of cellulose is an undesirable consequence of high carboxylic content.

The yield of a NFC sample is considered as the fraction in percentage of non-nanofibrillated and partially fibrillated fibres. The fibrillated fraction is separated from the non-fibrillated one by centrifugation. The individual nanofibrils are found in the supernatant, whereas non-fibrillated and partially fibrillated material remains in the precipitate at the bottom of the bottle. Thus, the yield of our NFC was 90.13 %. This can be considered as a high yield, though NFC with higher carboxylic content may present yields closer to 100 %.

Physical and morphological properties of nanopapers

The physical properties of all samples are summarized in Table 1. In general, the transition from paper to nanopaper produced thinner handsheets as the amount of NFC was increased. Samples entirely made of NFC were almost twice thinner and less bulky than those of neat eucalyptus fibres. The addition of NFC also gave denser papers, and 100 wt% NFC samples presented density values similar to those reported by other authors (Henriksson et al. 2008; Österberg et al. 2013).

Papers also became more transparent (less opaque) as the NFC content increased. This reduction in opacity is explained by the nanometric nature of NFC: since nanofibres have diameters below light's wavelength, an increase in transparency was expected. Samples with 100 wt% of NFC were not fully transparent due to the presence of fibres with micrometric size which were not completely fibrillated. Porosity is a parameter that describes the empty spaces (filled with air) between the fibres; nanofibrils tend to occupy these air-filled spaces among the larger fibres. Thus, paper becomes more compact, with a more continuous and homogenous structure. The reduction in porosity is an important feature because of its close relationship with mechanical properties: less-porous papers present higher strength due to an increase of hydrogen bonds, promoted by the high specific surface area of NFC. The porosity value of 20 % for 100 wt% NFC nanopapers is similar to that reported by Sehaqui et al. (2010) for nanopapers prepared also with a Rapid Köthen equipment. Dense nanopapers with low-porosity are interesting for applications where barrier properties are needed (Österberg et al. 2013).

Laser profilometry allowed understanding the surface characteristics of the papers and how they are

Table 1 Evolution of physical properties of papers and nanopapers with different NFC content

NFC content	Thickness (μm)	Density (kg/m^3)	Bulk (m^3/kg)	Opacity (%)	Porosity (%)	Roughness (μm)	
						Top side	Bottom side
0 % NFC	101 ± 1.20	640 ± 1.2	1,562	84.50 ± 0.01	57.30	4.66 ± 0.14	4.62 ± 0.26
25 % NFC	88 ± 0.23	730 ± 1.8	1,569	51.02 ± 0.02	51.30	4.13 ± 0.20	3.96 ± 0.13
50 % NFC	75 ± 0.15	810 ± 0.9	1,233	45.66 ± 0.01	46.00	3.05 ± 0.13	2.57 ± 0.12
75 % NFC	62 ± 0.18	950 ± 1.0	1,051	40.20 ± 0.01	36.66	2.23 ± 0.16	2.17 ± 0.44
100 % NFC	52 ± 0.01	1,200 ± 1.1	832	33.20 ± 0.01	20.00	1.10 ± 0.14	0.85 ± 0.11

affected by the NFC presence. Low values indicate smoother surfaces. Table 1 also presents the roughness determined for both sides of the papers. The bottom side column corresponds to the side in contact with the nitrocellulose membrane. The evolution of this parameter from papers made of large fibres to smoother nanopapers is significant. Paper made of large fibres presented similar roughness at both sides of the sheet; the difference in roughness between the two sides becomes wider as the amount of NFC increases. The lower roughness for bottom sides can be explained as a consequence of NFC being pressed against the flat membrane during the dewatering process.

In Fig. 2 SEM microphotographs of nanopapers with 50, 75 and 100 wt% of NFC at different magnifications are presented. This set of pictures shows how the main morphological features of nanopapers change with amount of NFC added. Picture C corresponds to handsheets with a 50 wt% of NFC content; the larger fibres are very conspicuous, with a random-in-the-plane distribution; large spaces appear between fibres, and these spaces are occupied by the NFC, though some NFC are also expected to be attached to the surface of larger fibres. Picture B shows a more homogeneous, smoother surface, which is important in printing papers (Sehaqui et al. 2011). Dense regions of NFC occupy the spaces between large fibres. Picture A belongs to 100 wt% NFC nanopaper; in this sample, the surface is very homogenous and smooth, with only a few larger fibres distributed within the nanopaper. The inset in this picture has an AFM image that gives some important morphological characteristics of nanopapers.

The nanometric nature of the NFC used in the present work is clear in the AFM picture; the width of the NFC was around 20–50 nm, which indicates that the NFC gel contains aggregates rather than single nanofibrils, since individual nanofibrils present widths in the range of 5 nm; the length of the NFC could not be determined through AFM imaging due to the dense physical entanglement of NFC where nanofibril ends were not visible. Another important feature of nanopapers is their porous structure. Pores are of irregular shape, not uniformly distributed, with diameters of up to 50 nm. A similar morphology has been reported by several authors (Henriksson et al. 2008; Chinga-Carrasco et al. 2013; Nogi et al. 2009; Chun et al. 2011).

Mechanical properties of nanopapers

Table 2 illustrates the evolution of mechanical properties of the samples. Tensile strength was doubled up after adding only 25 % of NFC to the slurry; the improvement continued almost linearly with subsequent addition of NFC. Nanopapers made out of 100 wt% of NFC presented the best tensile strength results.

The stress–strain curves of the nanopapers are shown in Fig. 3. A fairly linear elastic behaviour was observed at early deformations, with no structural damage. The next important feature is a yielding knee that corresponds to debonding of eucalyptus fibres (Sehaqui et al. 2011). Samples with 25 and 50 wt% of NFC have very similar curves. As the amount of NFC increases, this yielding knee was observed at higher stress. A linear plastic region comes after the yielding knee; stress and strain at break become higher in relation to the amount of NFC, except for the sample with 75 wt% of NFC, where the strain at break is somehow lower than the other samples. The fibre–fibre stress transmission in the plastic region is clearly enhanced by better bonding ability a formation of a three-dimension network (Chun et al. 2011) and higher intrinsic strength of NFC in comparison to

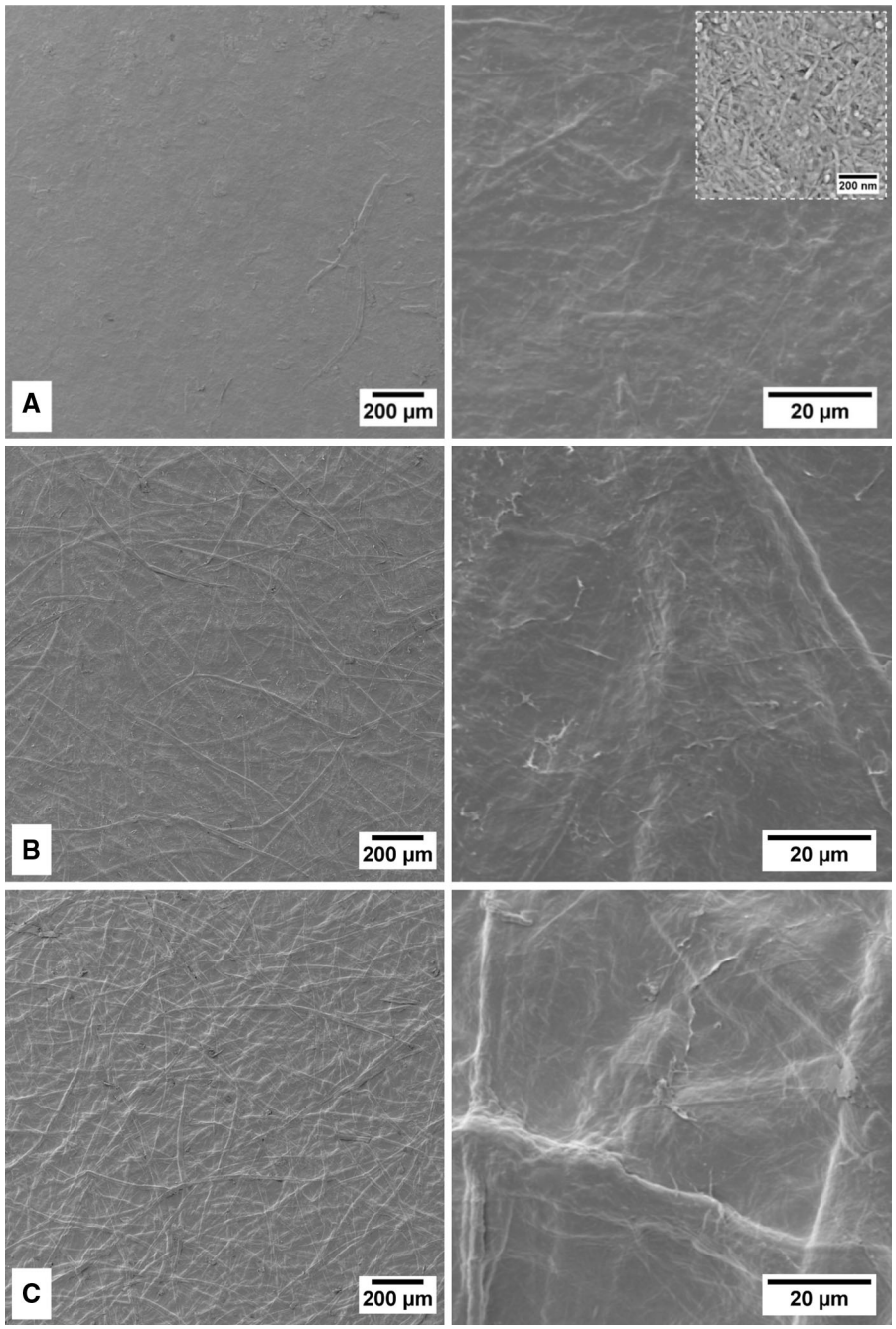

Fig. 2 SEM microphotography of the surface of nanopapers with 100, 75 and 50 wt% of NFC content (**a**–**c**, respectively). The *inset* in **a** shows an AFM image from the same sample exemplifying the nanofibrillated structure

larger fibres. Strength at break in the plastic region of cellulose fibres with polymerization degrees under 2,500 is a consequence of slippage of overextended cellulose chains, instead of breaking of covalent bonds expected at higher DP (Henriksson et al. 2008; Sehaqui et al. 2011).

The second column of Table 2 shows the evolution of Young's modulus; papers with a 25, 50 and 75 wt%

Table 2 Mechanical properties of nanopapers with different NFC content

NFC content	σ (MPa)	E (GPa)	Elastic limit (MPa)	ε (%)
0 % NFC	41.20 ± 2.32	2.85 ± 0.81	15.12 ± 1.01	0.65 ± 0.02
25 % NFC	82.98 ± 2.95	6.91 ± 0.25	23.47 ± 0.38	3.23 ± 0.21
50 % NFC	91.82 ± 4.45	8.20 ± 0.69	30.01 ± 0.61	3.24 ± 0.46
75 % NFC	113.48 ± 8.01	10.90 ± 0.34	36.51 ± 1.39	1.90 ± 0.14
100 % NFC	135.21 ± 18.28	11.90 ± 0.78	46.35 ± 1.32	3.59 ± 0.71

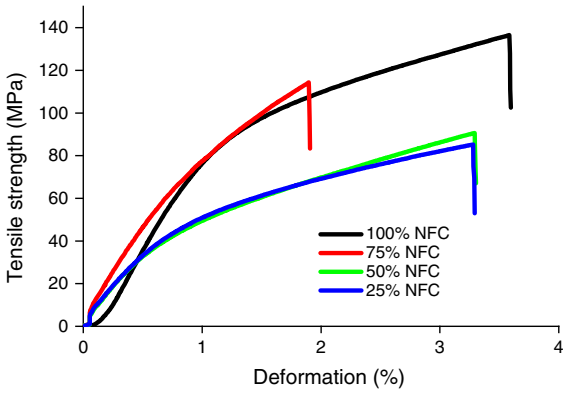

Fig. 3 Stress–strain curves of nanopapers with different NFC content

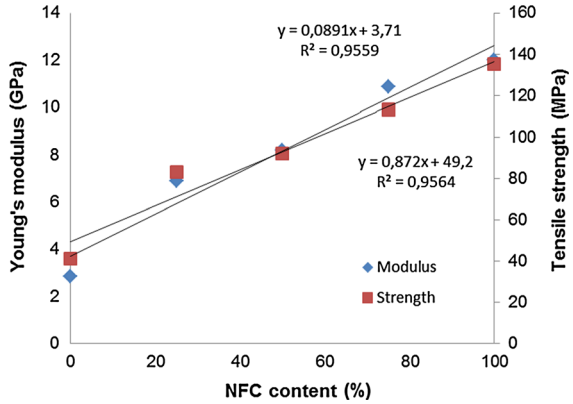

Fig. 4 Evolution of Young's modulus and tensile strength in relation to the NFC content

content of NFC increased rigidity up to 142, 188 and 282 %, respectively. Nanopapers with 100 wt% content of NFC presented the highest Young's modulus. It is known that Young's modulus of a fibre network depends on fibre orientation, number of bonds between fibres and intrinsic Young's modulus of a single fibre (Kulachenko et al. 2012). In nanopapers, NFC presents a random-in-the-plane orientation, as can be seen in SEM microphotography (Fig. 2), no matter the amount of NFC added. This fact greatly influences the ultimate tensile strength and Young's modulus of the nanopaper. The Young's modulus of a single, highly crystalline nanofibril has been reported to be between 30 and 250 GPa, depending on the author (Yano and Nakahara 2004; Zimmerman et al. 2004; Iwamoto et al. 2009; Saito et al. 2013; Alcala et al. 2013); this variation of results may be a consequence of the different sources of cellulose, methods of extraction and techniques applied to determine the strength and stiffness of the fibre. However, this high Young's modulus of a single nanofibril seems not to be reflected in nanopapers; though there is a clear, fairly linear increase in tensile strength and modulus in relation to the amount of NFC (Fig. 4), nanopapers of 100 wt% content of NFC have lower mechanical properties than expected if we consider the high intrinsic strength of single nanofibrils. In the case of nanopapers with a content equal or below to 50 wt% of NFC, the low Young's modulus could be the result of the presence of larger fibres inside the nanopaper; these larger fibres are less rigid than nanofibrils and develop tensile fracturing before NFC does when the nanopaper undergoes tensile stress; besides, the amount of hydrogen bonds between larger fibres is lower. At higher NFC content, however, the increase in mechanical properties is still far from that of a single nanofibril. In the present work, the Young's modulus of 11.9 GPa found in our nanopapers is very close to what has been reported by other authors (Henriksson et al. 2008; Chun et al. 2011; Österberg et al. 2013; Alcala et al. 2013).

Several theories have been developed to explain this fact. Saito et al. (2013) proposed that nanofibrils undergo structural damages in the fabrication of NFC, for example during the TEMPO-mediated oxidation, where the formation of –COOH groups on the nanofibrils' surface possibly reduces the intrinsic

strength of the nanofibrils. On the other hand, Kulachenko et al. (2012) explained that low Young's modulus of nanopapers can be a consequence of the variation of the intrinsic Young's modulus along the fibres and the three-dimensionality of the bonds within the nanopaper's structure.

Regarding the elastic limit, this parameter also increased along with the addition of NFC. On the other hand, the strain to failure presented first an increase until 50 wt% of NFC content. Then, a reduction was observed in nanopapers with 75 wt% of NFC and then the property increases again with a 100 wt% of NFC. The improvement of the overall handsheet's strength is a result of a high specific surface area of NFC, which promotes the formation of hydrogen bonding inside the paper's inner structure. Handsheets with NFC content below 50 % can be considered as nanocomposites where larger fibres are the matrix and NFC the filler. In this case, NFC forms a web-like network embedded among the larger fibres, filling the empty spaces within in the matrix. A part of the NFC is also supposed to attach to the rough surface of larger fibres, which accounts for the smoother surface of papers with high contents of NFC. In handsheets with a NFC content superior to 50 %, nanofibrils become the matrix and larger fibres can be considered as the filler. In this case, the improvement in mechanical properties was not affected by the presence of larger fibres with inferior mechanical properties due to the good interface between the NFC matrix and the larger fibres.

It is important to remark the impact that dispersion and drying have on the overall properties of nanopapers. A previous study from our research group denoted the importance of good dispersion in the final mechanical properties of NFC-reinforced paper (Alcala et al. 2013). In that study the improvement of paper's strength was achieved by only increasing the intensity of the dispersion step. The direct conclusion of this was that, by keeping the NFC-fibre mixture more time in the pulp disintegrator, the dispersion of the slurry was slightly improved. This produced a better contact between NFC and micro-sized fibres, hence boosting the number of hydrogen bonds formed during the drying step that ultimately are responsible for many of the final properties of nanopaper. In the aforementioned study, papers fabricated had a maximum NFC content of 12 wt%. It is possible that the same behaviour would be observed in paper sheets with higher contents of NFC like in the present work. The SEM microphotographs from Fig. 2 show that, in general, a good dispersion of NFC was achieved.

Regarding the drying step, the process has a great influence on the ultimate strength of nanopapers. Several methodologies are reported in the literature with varied results, from casting and drying at room temperature to vacuum drying. The Rapid–Köthen methodology used in the present study has been recognized as the fastest and easiest technique for fabrication of nanopaper sheets. Sehaqui et al. (2010), experimented on several drying methods and noted the effect on the ultimate tensile strength and Young's modulus, proving that the Rapid–Köthen equipment provided nanopaper sheets with better mechanical properties in comparison to suspension casting, hot drying and hot pressing. The main advantage of using the Rapid–Köthen is its fast water removal. Besides, since the nanopapers are constraint between the two clamps, shrinkage and wrinkling of the sheet are prevented. Moreover, the technique favours a homogenous in-plane orientation of the nanofibres which accounts also for the high mechanical properties and high density of nanopapers.

Finally, the high degree of fibrillation in NFC's has also an important effect on the characteristics of nanopapers. NFC with high degree of fibrillation, indirectly quantified here by transmittance and yield of fibrillation, promotes good dispersion of nanofibres and therefore a uniform distribution of the defects and failure starters (i.e. pores) within the nanopaper structure.

Conclusions

The results presented in this work show that it is possible to prepare a wide variety of papers with different NFC content. These papers or nanopapers could be prepared in a Rapid Köthen-like equipment. Nanopapers become denser, bulkier and smoother as more NFC is added and nanopapers made only of NFC presented porosity values similar to those reported in the literature; opacity was greatly reduced in accordance to the amount of NFC. The SEM microphotography showed that the structure of papers and nanopapers becomes smoother and with a more homogenous appearance as the amount of NFC increases. AFM imaging from 100 wt% of NFC showed nanofibril aggregates with diameters in the

range of 20–50 nm that form a porous structure of entangled NFC.

The evolution of mechanical properties is also in relation to the amount of NFC in the nanopaper. Both tensile strength and Young's modulus increased linearly after more NFC was added to the paper. Nanopapers of 100 wt% of NFC presented the best strength results. NFC also induced an improvement in the elastic limit. The strain at failure had an irregular behaviour, showing first a steady increase in samples with up to 50 wt% of NFC, followed by a reduction in nanopapers with 75 wt% of NFC, whereas samples fully made of NFC presented the highest value for strain at break.

The superior properties of nanopapers in comparison to normal papers is a result of the high adhesion between nanofibrils thanks to hydrogen-bonding, their high intrinsic mechanical properties and their ability to form homogenous, compact structures where morphological defects are more regularly distributed in contrast to larger fibres. Moreover, the dependence of paper strength on the amount of NFC indicates that the ultimate tensile strength relies on nanofibril breakage.

Acknowledgments The authors are thankful to the Spanish Ministry of Science and Innovation for the financial support given by the projects CTQ2010-21660-C03-03 and CTM2011-28506-C02-01 to develop this study.

References

Ahola S, Österberg M, Laine J (2008) Cellulose nanofibrils adsorption with poly(amideamine) epichlorohydrin studied by QCM-D and application as a paper strength additive. Cellulose 15:303–314

Alcala M, González I, Boufi S, Vilaseca F, Mutjé P (2013) All-cellulose composites from unbleached hardwood kraft pulp reinforced with nanofibrillated cellulose. Cellulose 20(6):2909–2921

Alila S, Besbes I, Rei Vilar M, Mutjé P, Boufi S (2013) Non-woody plants as raw materials for production of microfibrillated cellulose (MFC): a comparative study. Ind Crops Prod 41:250–259

Andresen M, Stenstad P, Moretro T, Langsrud S, Syverud K, Johansson LS, Stenius P (2007) Nonleaching antimicrobial films prepared from surface-modified microfibrillated cellulose. Biomacromolecules 8(7):2149–2155

Besbes I, Alila S, Boufi S (2011) Nanofibrillated cellulose from TEMPO-oxidized eucalyptus fibres: effect of the carboxyl content. Carbohydr Polym 84(3):975–983

Carrasco F, Mutjé P, Pèlach MA (1996) Refining of bleached cellulosic pulps: characterization by application of the colloidal titration technique. Wood Sci Technol 30(4):227–236

Chinga-Carrasco G (2013) Optical methods for the quantification of the fibrillation degree of bleached MFC materials. Micron 48:42–48

Chinga-Carrasco G, Averianova N, Gibadullin M, Petrov V, Leirset I, Syverud K (2013) Micro-structural characterisation of homogeneous and layered MFC nano-composites. Micron 44:331–338

Chun S-J, Lee S-Y, Doh G-H, Lee S, Kim JH (2011) Preparation of ultrastrength nanopapers using cellulose nanofibrils. J Ind Eng Chem 17:521–526

Dang Z, Zhang J, Ragauskas AJ (2007) Characterizing TEMPO-mediated oxidation of ECF bleached softwood kraft pulps. Carbohydr Polym 70:310–317

Dufresne A, Cavaillé J-Y, Vignon MR (1997) Mechanical behaviour of sheets prepared from sugar beet cellulose microfibrils. J Appl Polym Sci 64(6):1185–1194

Fang Z, Zhu H, Preston C, Han Z, Li Y, Lee S, Chai X, Chen G, Hu L (2013) Highly transparent and writable wood all-cellulose hybrid nanostructured paper. J Mater Chem C 1:6191–6197

González I, Boufi S, Pelach MA, Alcalà M, Vilaseca F, Mutjé P (2012) Nanofibrillated cellulose as paper additive in eucaliptus pulps. Bioresources 7(4):5167–5180

González I, Alcalà M, Arbat G, Vilaseca F, Mutje P (2013a) Suitability of rapeseed chemithermomechanical pulp as raw material in papermaking. Bioresources 8(2):1697–1708

González I, Vilaseca F, Alcalà M, Pèlach MA, Boufi S, Mutjé P (2013b) Effect of the combination of biobeating and NFC on the physico-mechanical properties of paper. Cellulose 20:1425–1435

Henriksson M, Berglund L, Isaksson P, Lindstrom T, Nishino T (2008) Cellulose nanopaper structures of high tughness. Biomacromolecules 9:1579–1585

Henriksson M, Fogelström L, Berglund LA, Johansson M, Hult A (2011) Novel nanocomposite concept based on cross-linking of hyperbranched polymers in reactive cellulose nanopaper templates. Compos Sci Technol 71:13–17

Isogai A, Saito T, Hayaka F (2011) TEMPO-oxidized cellulose nanofibres. Nanoscale 3:71–85

Iwamoto S, Kai W, Isogai A, Iwata T (2009) Elastic modulus of single cellulose microfibrils from tunicate measured by atomic force microscopy. Biomacromolecules 9:2571–2576

Kulachenko A, Denoyelle T, Galland S, Lindström SB (2012) Elastic properties of cellulose nanopaper. Cellulose 19:793–807

Mutjé P, Pèlach MA, García JC, Presta S, Vilaseca F, Jiménez L (2006) Comparison of cationic demand between olive wood organosolv pulp and eucaliptus kraft pulp. Process Biochem 41:1602–1607

Nogi M, Iwamoto S, Nakagaito AN, Yano H (2009) Optically transparent nanofibre paper. Adv Mater 21:1595–1598

Österberg M, Vartiainen J, Lucenius J, Hippi U, Seppala J, Serimaa R, Laine J (2013) A fast method to produce strong NFC films as a platform for barrier and functional materials. Appl Mater Interfaces 5:4640–4647

Saito S, Kimura S, Nishiyama Y, Isogai A (2007) Cellulose nanofibers prepared by TEMPO-mediated oxidation of native cellulose. Biomacromolecules 8:2485–2491

Saito T, Kurumae R, Wohlert J, Berglund LA, Isogai A (2013) An ultrastrong nanofibrillar biomaterial: the strength of single cellulose nanofibrils revealed via sonication-induced fragmentation. Biomacromolecules 14:248–253

Sehaqui H, Liu A, Zhou Q, Berglund L (2010) Fast preparation procedure for large, flat cellulose and cellulose/inorgànic nanopaper structures. Biomacromolecules 11:2195–2198

Sehaqui H, Allais M, Zhou Q, Berglund L (2011) Wood cellulose biocomposites with fibrous structures at micro- and nano-scale. Compos Sci Technol 71:382–387

Siró I, Plackett D (2010) Microfibrillated cellulose and new nanocomposite materials: a review. Cellulose 17:459–494

Taipale T, Österberg M, Nykänen A, Ruokolainen J, Laine J (2010) Effect of microfibrillated cellulose and fines on the drainage of kraft pulp suspensions and paper strength. Cellulose 17:1005–1020

Varanasi S, Batchelor WJ (2013) Rapid preparation of cellulose nanofibre sheet. Cellulose 20:211–215

Yano H, Nakahara S (2004) Bio-composites produced from plant microfiber bundles with nanometer unit web-like network. J Mater Sci 39:1635–1638

Zimmerman T, Pöhler E, Geiger T (2004) Cellulose fibrils for polymer reinforcement. Adv Eng Mater 6:754–761